Short communication

Insight in the relationship between magnetism of stoichiometric spinel ferrites and their catalytic activity

Ji Ma, Chunting Liu, Kezheng Chen*

Lab of Functional and Biomedical Nanomaterials, College of Materials Science and Engineering, Qingdao University of Science and Technology, Qingdao 266042, China

ABSTRACT

In this work, spinel ferrites were chosen as prototype systems for oxidative dehydrogenation of 1-butene to address the long-standing issue that whether there is a correlation between catalytic and magnetic properties of magnetic catalysts. Under zero magnetic field, the conversion was the largest for $NiFe_2O_4$ (74.5 mol%) and the least for $ZnFe_2O_4$ (12.6 mol%), with no quantative relationship between magnetism and catalytic activity. In contrast, under a magnetic field of 1603 Oe, the largest and least conversion values changed to 86.6 and 13.5 mol% for $MgFe_2O_4$ and $ZnFe_2O_4$, respectively, and these values exhibited an inverse Gauss relation with initial susceptibility.

1. Introduction

As is known, magnetic catalysts can be separated from the reactants and byproducts in a liquid-phase reaction via exerting an external magnetic field [1–3]. Such magnetically driven separation makes the recovery of catalysts much easier and more efficient than by cross-flow filtration and centrifugation, especially when the catalysts are in the sub-micrometer size range [4,5]. In this regard, magnetic catalysts can combine advantages of high dispersion and reactivity with easy separation. Apart from contributing to separation, the inherent magnetism of catalysts may also contribute to their catalytic activity to some extent. Up to now, mounting experimental evidence has been revealing the relevance between magnetism and catalytic activity [6–10]. Despite these endeavors, research on their quantitative correlation rather than simply qualitative description is still in its very infant stage.

A major hurdle to a more definitive understanding of their quantitative relationship is the presence of myriad influence factors including stoichiometric ratio of constituent elements, surface groups as well as particle size and shape, let alone numerous pertinent parameters with regard to elemental doping and catalytic conditions [11,12]. Keeping these aspects in mind and in quest of the distinct functional relation between magnetic and catalytic parameters, in this work, we fabricated various stoichiometric spinel ferrites, MFe_2O_4, wherein M denoted metal ions including divalent zinc (Zn(II)), cadmium (Cd(II)), manganese (Mn(II)), iron (Fe(II)), magnesium (Mg(II)), copper (Cu(II)), cobalt (Co(II)) and nickel (Ni(II)). On account of the identical synthetic route

for all these spinel ferrites, their particle size, shape and surface groups were seen as the same. Besides, the oxidative dehydrogenation of 1-butene was chosen as a model catalytic reaction and the catalytic conversion of 1-butene to butadiene, CO_2 and 2-butene conversions were conducted under equal conditions. Apart from these considerations, an external magnetic field (ca. 1603 Oe) was applied during the oxidative dehydrogenation reaction and the results that were obtained with and without such a magnetic field were compared and used as compelling evidence to establish the quantitative relationship between magnetism and catalytic activity.

2. Experimental

2.1. Synthesis of stoichiometric spinel ferrites

All reagents in synthesis were analytically pure and used as received from Sinopharm Chemical Reagent Co., Ltd. (China) without further purification. To synthesize stoichiometric MFe_2O_4, all metal ions are supplied by their chlorides and the molar concentration ratio between divalent metal chlorides and ferric chloride was initially set as 0.5, which could be further slightly adjusted so as to achieve an ideal stoichiometric ratio in final products. In a typical experiment, any one of divalent metal chlorides (including $ZnCl_2$, $CdCl_2$, $MnCl_2$, $FeCl_2$, $MgCl_2$, $CuCl_2$, $CoCl_2$ and $NiCl_2$) was mixed with 2 mmol $FeCl_3$ reagent and fully dissolved into 30 mL ethylene glycol. After that, 8 mmol potassium hydroxide powders were added in while keeping vigorous agitation. The stock solution was then transferred into a Teflon-lined stainless-

---

* Corresponding author.
  E-mail address: kchen@qust.edu.cn (K. Chen).

steel autoclave with a capacity of 50 mL for solvothermal treatment at 180 °C for 2 h. After the autoclave was cooled down to room temperature naturally, the sediment was collected by centrifugation, repeatedly washed with deionized water and absolute ethanol, and finally dried at 60 °C for 4 h. Subsequently, the dried powder was ground and further annealed in argon flow at 500 °C for 2 h using a tube furnace. Eventually, the as-obtained powder was repeatedly washed with deionized water until it was chlorine free, as tested with a 1 mol L^{-1} silver nitrate solution and dried in air at 60 °C overnight.

2.2. Characterization

Elemental composition of these as-synthesized spinel ferrites was determined by atomic absorption spectroscopy (AAS) with a Perkin-Elmer 2380 apparatus. Prior to the analysis, 50 mg of spinel ferrites were dissolved into 0.5 mol L^{-1} HNO$_3$ aqueous solution under constant mechanical agitation for 2 h at 70 °C. AAS measurements were performed in triplicate. Transmission -electron microscope (TEM) images were obtained on the JEOL 2010 TEM with an operating voltage of 200 kV. Magnetic measurements were conducted using a commercial superconducting quantum interference device magnetometer (SQUID, MPMS-XL5) at 300 K. The initial magnetization curve was obtained by applying a magnetic field from 0 to +50 kOe.

2.3. Catalytic experiments

The catalytic oxidative dehydrogenation of 1-butene was performed with 200 mg of spinel ferrites in a conventional continuous flow reactor. In order to exert a magnetic field during the catalytic reaction, a commercial Al-Ni-Co magnet with a Curie temperature of 860–900 °C and magnetic field strength of 1603 Oe (measured by a hand-held digital Tesla meter, YA1-WT10C) was put underneath the porcelain boat that held ferrite samples. Before the catalytic reaction, each ferrite sample was heated to 420 °C and maintained at that temperature under airflow of 30 cm^3 min^{-1} for 2 h so as to produce a totally oxidized surface. Afterwards, a blend of 5 mol% of 1-butene, 5 mol% of oxygen and 90 mol% of helium was fed into the reactor at a total flow rate of 60 cm^3 min^{-1}. The reaction products were finally analyzed on-line in a Varian Aerograph 3700 gas chromatograph equipped with a 30 ft. column of 23%SP-1700 on 80/100 Chromosorb PAW and a thermal conductivity-based detector. As a comparison, the same catalytic procedure was conducted without using the commercial Al-Ni-Co magnet.

3. Results and discussion

To find out quantitative relation between magnetism of spinel ferrites and their catalytic activity for oxidative dehydrogenation of 1-butene, several non-negligible interfering factors should be considered and standardized in advance. Probably, the stoichiometric ratio between divalent metal ions and ferric ion in ferrites is the first and foremost factor because a slight change of this ratio may result in significantly different catalytic activity [13–15]. In this scenario, standardizing this ratio to an ideal value of 0.5 is a prerequisite in the following investigation, even though its realization is cumbersome at nanometric scale. To this end, we repeatedly utilize atomic absorption spectroscopy to determine the elemental composition of the as-synthesized ferrites, and attempt to adjust molar concentration of divalent metal chlorides before synthesis if the calculated stoichiometric values in final ferrites deviate from 0.5. Table 1 gives elemental composition of divalent metal ions and ferric ion by a weight percentage for various spinel ferrites, and further provides their corresponding atomic ratios that exhibit no substantial deviation from the ideal value of 0.5.

Under the premise of near-stoichiometric character of these spinel ferrites, further consideration is given to the standardization of particle size and shape, in that these two factors may also exert great impact on catalytic activity [16–21]. To this aim, TEM characterization is

Table 1
Chemical element composition of ferrite catalysts.

Catalysts	M	Elemental composition (wt%)		M/Fe atomic ratio
		Fe	M	
MFe$_2$O$_4$	Zn(II)	46.2	27.1	0.505
	Cd(II)	38.7	38.5	0.498
	Mn(II)	48.2	23.7	0.500
	Fe(II)	48.1	24.0	0.500
	Mg(II)	55.9	12.1	0.505
	Cu(II)	46.7	26.4	0.500
	Co(II)	47.6	25.2	0.502
	Ni(II)	47.7	25.1	0.502

conducted and the obtained images are presented in Fig. S1. Obviously, most of particles in these ferrites are spherical-like, although some particles are irregular, as if they were formed by aggregation of two or three virgin particles. Additionally, the different contrast among particles is due to the different electron penetration efficiency on the TEM sample, revealing an apparent agglomeration of ferrites particles that can be ascribed to slow solvent evaporation when drying during TEM sample preparation. The average sizes of these ferrites particles can be estimated by statistically counting a hundred isolated or well-defined particles, as shown in Fig. S2. The sizes of ZnFe$_2$O$_4$, CdFe$_2$O$_4$, MnFe$_2$O$_4$, Fe$_3$O$_4$, MgFe$_2$O$_4$, CuFe$_2$O$_4$, CoFe$_2$O$_4$, NiFe$_2$O$_4$ distribute around peak values of 8 nm (Fig. S2a), 8 nm (Fig. S2b), 9 nm (Fig. S2c), 7 nm (Fig. S2d), 7 nm (Fig. S2e), 9 nm (Fig. S2f), 7 nm (Fig. S2g), 7 nm (Fig. S2h), respectively, and the width of their distribution at half-maximum is generally around 2 nm. Collectively, the shape and size of these MFe$_2$O$_4$ (M stands for Zn, Cd, Mn, Fe, Mg, Cu, Co and Ni) particles can be readily standardized into consistency by performing exactly the same synthetic route for all these spinel ferrites.

After standardizing these interfering factors, catalytic oxidative dehydrogenation of 1-butene is conducted in two separate ways: non-magnetic and magnetic. Their difference lies in whether a commercial Al-Ni-Co magnet is placed under the porcelain boat that held ferrite powders. Given that our catalytic reaction temperature is 420 °C, Al-Ni-Co magnet with high working temperature of ca. 900 °C is appreciably more qualified than other common magnets such as ferrite magnets (ca. 350 °C), Nd-Fe-B magnets (ca. 200 °C) and SmCo magnets (ca. 350 °C). Fig. 1a and 3b show the conversion of 1-butene over different ferrite catalysts without and with the aid of an Al-Ni-Co magnet during the oxidative dehydrogenation reaction, respectively. It is observed that nearly all spinel ferrites, except for NiFe$_2$O$_4$, exhibit much higher conversion values when the Al-Ni-Co magnet is applied. Although the enhancing degree of conversion is quite different for these ferrite catalysts, it strongly evidences that prompting their magnetic responses by an external magnetic field can boost their catalytic activity. Moreover, in nonmagnetic case, the conversion of 1-butene is observed to be the highest for NiFe$_2$O$_4$ (74.5 mol%), followed by CoFe$_2$O$_4$ (55.8 mol%), CuFe$_2$O$_4$ (43.4 mol%), MgFe$_2$O$_4$ (32.1 mol%) and then Fe$_3$O$_4$ (22.7 mol%), MnFe$_2$O$_4$ (17.9 mol%), CdFe$_2$O$_4$ (14.3 mol%), and ZnFe$_2$O$_4$ (12.6 mol%). In contrast, after applying a magnetic field, the conversion of 1-butene follows the sequence of MgFe$_2$O$_4$ (86.6 mol%), CuFe$_2$O$_4$ (80.3 mol%), CoFe$_2$O$_4$ (68.5 mol%), NiFe$_2$O$_4$ (55.7 mol%), Fe$_3$O$_4$ (42.9 mol%), MnFe$_2$O$_4$ (28.2 mol%), CdFe$_2$O$_4$ (18.7 mol%), and ZnFe$_2$O$_4$ (13.5 mol%).

The mechanism of the oxidative dehydrogenation of 1-butene to butadiene and CO$_2$ is highly relevant to the activity of Fe(III)-cation sites. The charge transfer from Fe(III) cations to oxygen anions in the Fe−O bond makes the oxygen bonded to Fe(III) cation basic [22]. Therefore, the acid-base type dissociation of the C−H bond for the butene activation to produce butadiene and CO$_2$ is favorable [23]. From the atomic perspective, a unit cell in any spinel ferrite contains 32 oxygen anions that form a face centered cubic lattice. This configuration yields 64 tetrahedral interstices (A sites) and 32 octahedral
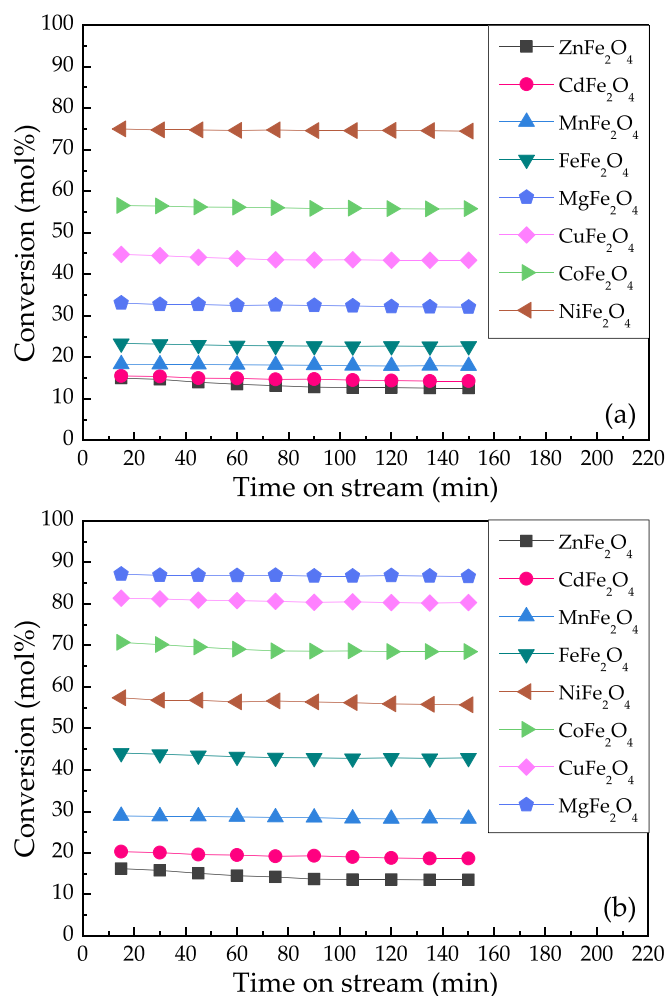
Fig. 1. (Color online) Conversion of 1-butene over ferrite catalysts: (a) without and (b) with the presence of an external magnetic field during the oxidative dehydrogenation reaction.

Fig. 2. (Color online) (a) 1-butene conversion values for ferrite catalysts with various divalent metal ions under zero magnetic fields. The solid line is guideline for eyes. (b) Correlation between the conversion of 1-butene and initial susceptibility of ferrite catalysts with the presence of an external magnetic field during the catalytic reaction. The solid line is a fitting result according to the inverse Gauss function.

interstices (B sites). Sixteen Fe(III) ions separately occupy 8 of 64 A sites and 8 of 32 B sites. The tendency to occupy A sites for divalent metal ions is known to follow the order (from weak to strong): Ni(II), Co(II), Cu(II), Mg(II), Fe(II), Mn(II), Cd(II), Zn(II), which bears striking similarities with the observed conversion order in the nonmagnetic case. This finding clearly indicates the existence of a correlation between occupancy tendency of divalent metal ions and catalytic conversion of 1-butene. Unfortunately, this correlation as depicted in Fig. 2a is hard to quantify mainly because the occupancy tendency is too qualitative to be quantitatively described. The underlying physical cause for this correlation should have something to do with the matching degree of characteristic times. To be specific, it is mostly accepted that any spinel ferrite merely exposes B sites at its particle surface [24]. At the reaction temperature of 420 °C, all spinel ferrites in this study exhibit paramagnetism and the Fe(III) ions in B sites rotate rapidly at random with a characteristic time of few nanoseconds. On the other hand, 1-butene molecules are dynamically adsorbed and desorbed to the particle surface within a characteristic time of several microseconds at 420 °C. Therefore, the 1-butene molecules cannot sense the specific direction of Fe(III) magnetic moment in ferrite because the latter can rotate in all possible directions within the characteristic time of the former. However, things have changed as increasing the occupancy tendency of divalent metal ions to B sites. The more divalent cations occupy B sites, the more Fe(III) ions squeeze into A sites. These extra Fe(III) ions with its 3d electrons partially filled in the A sites will pin the nearby
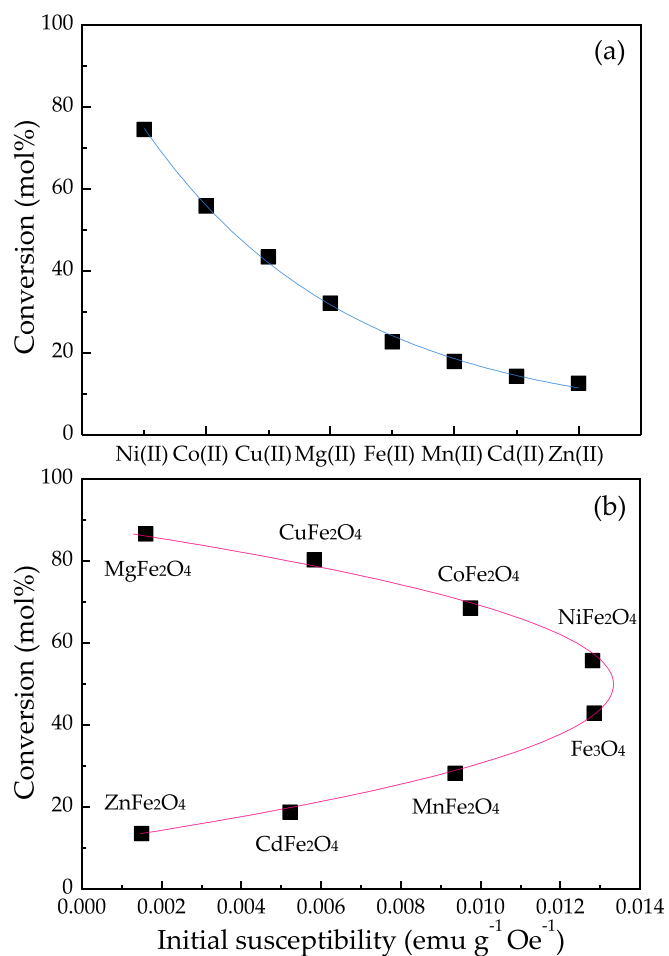
magnetic moments in B sites via an antiferromagnetic interaction [25–27], and hence slowing down the rotation of Fe(III) magnetic moment in B sites. Apparently, this pinning effect will increase the matching degree of the above two characteristic times, and become more and more prominent as increasing the tendency of divalent metal ions to occupy B sites. This means the 1-butene molecules near e.g. NiFe$_2$O$_4$ surfaces can more easily detect the magnetic moments produced by non-paired 3d electrons and interact with them, and thus running more efficient oxidative dehydrogenation reaction than that in the case of ZnFe$_2$O$_4$.

Based on the above analysis, the comparability between the two characteristic times, including the time of the rotation of Fe(III) magnetic moment in surface-exposed B sites and the time of dynamic adsorption/desorption of 1-butene molecules near particle surface, is of great importance to the enhancement of 1-butene conversion during catalytic reaction. Notwithstanding a much longer time required for adsorbing and desorbing 1-butene molecules around particle surface in normal case, pinning the Fe(III) magnetic moment in B sites is an effectual approach to slow down its thermal rotation and hence making these two characteristic times comparable. As stated in the preceding section, introducing divalent metal ions in the B sites can effectively pin the target Fe(III) magnetic moment. Not only that, but applying an external magnetic field can also realize this pinning aim. At the reaction temperature of 420 °C, the strong thermal agitation prompts Fe(III)

magnetic moments to rotate at random in time at frequencies of the order of Gigahertz, whereas the applied external magnetic field tends to align and fix them along the field direction. It should be noted that if these Fe(III) magnetic moments are firmly pinned in the applied magnetic field, then the characteristic time regarding the rotation of these magnetic moments is greatly enhanced and even far surpass the time of molecules adsorption/desorption around the particle surface. That being the case, a mismatch between these two characteristic times re-occurs and once again lowers the conversion of 1-butene. That is what happened for the $NiFe_2O_4$ case, in which the conversion of 1-butene decreases from 74.5 mol% to 55.7 mol% when an external magnetic field is applied during the oxidative dehydrogenation reaction. The synergy of divalent-ion pinning and magnetic-field pinning makes the conversion of 1-butene behave completely different with regard to the nonmagnetic and magnetic catalytic reaction (Fig. 1a and b). Further, the initial susceptibility is used as a metric to quantify this synergetic effect. By measuring magnetization curves (*M* vs. *H*) of spinel ferrites and then taking derivatives of them, the data values at the origin from the d*M*/d*H* vs. *H* curves are taken as the initial susceptibility. The plot of conversion value of 1-butene and initial susceptibility of ferrite catalysts is shown in Fig. 2b, from which one can observe a clear-cut functional relation between the two. With the help of nonlinear fitting, this correlation can be nicely described by an inverse Gauss function, that is, $(C - C_0)^2 \propto \ln(\chi - \chi_0)$. Here, *C* and χ denote the conversion value of 1-butene and initial susceptibility of ferrite catalysts, respectively. The parameters with subscript "0" refer to undetermined constants that are highly relevant to max values of *C* and χ. This finding can not only predict conversion value of 1-butene based on the measured initial susceptibility of ferrite catalysts, but also unlock the quantitative investigation on the relationship between magnetism and catalytic activity in magnetic catalysis field. Although this quantitative relationship may not be versatile for any catalytic reaction using any type of magnetic catalyst, at least, it will have certain reference values to study the influence of many other factors while modifying this functional correlation.

4. Conclusions

In summary, a series of stoichiometric spinel ferrites, including $ZnFe_2O_4$, $CdFe_2O_4$, $MnFe_2O_4$, Fe_3O_4, $MgFe_2O_4$, $CuFe_2O_4$, $CoFe_2O_4$ and $NiFe_2O_4$, were synthesized via an identical solvothermal route. These ferrites were of similar spherical-like shape and uniform particle size (viz. 7–9 nm), and thus they were chosen as an ideal prototype system to find out the possible correlation between magnetism and catalytic activity. By using these ferrites as catalysts in oxidative dehydrogenation of 1-butene, two main conclusions were drawn:

(a) The occupation tendency of metal ions in tetrahedral and octahedral sites played a decisive role on the converison of 1-butene with absence of Al-Ni-Co magnet during the catalytic reaction. The more divalent metal ions occupied octahedral sites, the more obvious the pinning effect on Fe(III) magnetic moments in these sites, and the better matching of characteristic times and finally larger conversion value.

(b) With the help of an external magnetic field, the Fe(III) magnetic moments were readily fixed along the field direction, and hard to rotate at random under thermal agitation. The synergy of divalent-ion pinning and magnetic-field pinning made the conversion of 1-butene exhibit an inverse Gauss relation to the initial susceptibility of ferrite catalysts.

Declaration of Competing Interest

None.

Appendix A. Supplementary data

Supplementary data to this article can be found online at https://doi.org/10.1016/j.catcom.2020.105986.

References

[1] X. Li, K. Cui, Z. Guo, T. Yang, Y. Cao, Y. Xiang, H. Chen, M. Xi, Heterogeneous Fenton-like degradation of tetracyclines using porous magnetic chitosan microspheres as an efficient catalyst compared with two preparation methods, Chem. Eng. J. 379 (2020) 122324.

[2] S. Neamani, L. Moradi, M. Sun, Synthesis of magnetic hollow mesoporous N-doped silica rods as a basic catalyst for the preparation of some spirooxindole-1,4-dihydropyridine derivatives, Appl. Surf. Sci. 504 (2020) 144466.

[3] T. Su, J. Zeng, H. Gao, L. Jiang, X. Bai, H. Zhou, F. Xu, One-pot synthesis of a chemically functional magnetic carbonaceous acid catalyst for fermentable sugars production from sugarcane bagasse, Fuel 262 (2020) 116512.

[4] A.M. Chávez, R.R. Solís, F.J. Beltrán, Magnetic graphene TiO_2-based photocatalyst for the removal of pollutants of emerging concern in water by simulated sunlight aided photocatalytic ozonation, Appl. Catal. B Environ. 262 (2020) 118275.

[5] B. Ou, J. Wang, Y. Wu, S. Zhao, Z. Wang, Efficient removal of Cr (VI) by magnetic and recyclable calcined CoFe-LDH/g-C_3N_4 via the synergy of adsorption and photocatalysis under visible light, Chem. Eng. J. 380 (2020) 122600.

[6] G.E. Gomez, E.V. Brusau, J. Sacanell, G.J.A.A. Soler Illia, G.E. Narda, Insight into the metal content-structure-property relationship in lanthanide metal-organic frameworks: optical studies, magnetism, and catalytic performance, Eur. J. Inorg. Chem. (2018) 2452–2460.

[7] J.A. Toledo-Antonio, N. Nava, M. Martínez, X. Bokhimi, Correlation between the magnetism of non-stoichiometric zinc ferrites and their catalytic activity for oxidative dehydrogenation of 1-butene, Appl. Catal. A Gen. 234 (2002) 137–144.

[8] V. Belessi, D. Lambropoulou, I. Konstantinou, R. Zboril, J. Tucek, D. Jancik, T. Albanis, D. Petridis, Structure and photocatalytic performance of magnetically separable titania photocatalysts for the degradation of propachlor, Appl. Catal. B Environ. 87 (2009) 181–189.

[9] D. Beydoun, R. Amal, G.K.C. Low, S. McEvoy, Novel photocatalyst: titania-coated magnetite. activity and photodissolution, J. Phys. Chem. B 104 (2000) 4387–4396.

[10] Y. Gao, B. Chen, H. Li, Y. Ma, Preparation and characterization of a magnetically separated photocatalyst and its catalytic properties, Mater. Chem. Phys. 80 (2003) 348–355.

[11] Z.Y. Zhou, N. Tian, J.T. Li, I. Broadwell, S.G. Sun, Nanomaterials of high surface energy with exceptional properties in catalysis and energy storage, Chem. Soc. Rev. 40 (2011) 4167–4185.

[12] V. Polshettiwar, R. Luque, A. Fihri, H. Zhu, M. Bouhrara, J.M. Basset, Magnetically recoverable nanocatalysts, Chem. Rev. 111 (2011) 3036–3075.

[13] A. Goyal, S. Kapoor, P. Samuel, V. Kumar, S. Singhal, Facile protocol for reduction of nitroarenes using magnetically recoverable $CoM_{0.2}Fe_{1.8}O_4$ (M= Co, Ni, Cu and Zn) ferrite nanocatalysts, RSC Adv. 5 (2015) 51347–51363.

[14] Y. Feng, C. Liao, K. Shih, Copper-promoted circumneutral activation of H_2O_2 by magnetic $CuFe_2O_4$ spinel nanoparticles: mechanism, stoichiometric efficiency, and pathway of degrading sulfanilamide, Chemosphere 154 (2016) 573–582.

[15] A. Shabbir, S. Ajmal, M. Shahid, I. Shakir, P.O. Agboola, M.F. Warsi, Zirconium substituted spinel nano-ferrite $Mg_{0.2}Co_{0.8}Fe_2O_4$ particles and their hybrids with reduced graphene oxide for photocatalytic and other potential applications, Ceram. Int. 45 (2019) 16121–16129.

[16] H. Chen, S. Liu, J. Yin, X. Gao, Z. Tao, B. Wu, H. Xiang, Y. Yang, Y. Li, The influence of size and shape of Pd nanoparticles on the performances of Pd/Beta catalysts for n-heptane hydroisomerization, ChemCatChem 11 (2019) 3542–3551.

[17] M. Mandić, B. Todić, L. Živanić, N. Nikačević, D.B. Bukur, Effects of catalyst activity, particle size and shape, and process conditions on catalyst effectiveness and methane selectivity for Fischer-Tropsch reaction: a modeling study, Ind. Eng. Chem. Res. 56 (2017) 2733–2745.

[18] M. Abbas, Z. Chen, J. Chen, Shape- and size-controlled synthesis of Cu nanoparticles wrapped on RGO nanosheet catalyst and their outstanding stability and catalytic performance in the hydrogenation reaction of dimethyl oxalate, J. Mater. Chem. A 6 (2018) 19133–19142.

[19] S. Kolitcheff, E. Jolimaitre, A. Hugon, J. Verstraete, M. Rivallan, P.L. Carrette, F. Couenne, M. Tayakout-Fayolle, Tortuosity and mass transfer limitations in industrial hydrotreating catalysts: effect of particle shape and size distribution, Catal. Sci. Technol. 8 (2018) 4537–4549.

[20] M. Miyake, K. Miyabayashi, Shape and size controlled Pt nanocrystals as novel model catalysts, Catal. Surv. Jpn. 16 (2012) 1–13.

[21] H. Kotani, R. Hanazaki, K. Ohkubo, Y. Yamada, S. Fukuzumi, Size- and shape-dependent activity of metal nanoparticles as hydrogen-evolution catalysts: mechanistic insights into photocatalytic hydrogen evolution, Chem. Eur. J. 17 (2011) 2777–2785.

[22] J.A. Toledo, P. Bosch, M.A. Valenzuela, A. Montoya, N. Nava, Oxidative dehydrogenation of 1-butene over Zn-Al ferrites, J. Mol. Catal. A Chem. 125 (1997)

      53–62.

[23] D.J. Hucknall, Selective Oxidation of Hydrocarbons, Academic Press, New York, NY, 1974, p. 75.

[24] J.P. Jacobs, A. Maltha, J.G.H. Reintjes, J. Drimal, V. Ponec, H.H. Brongersma, The surface of catalytically active Spinels, J. Catal. 147 (1994) 294–300.

[25] G.M. Bancroft, M.D. Osborne, M.E. Fleet, Next-nearest neighbour effects in the

Mössbauer spectra of Cr-spinels: an application of partial quadrupole splittings, Solid State Commun. 47 (1983) 623–625.

[26] J.S. Smart, The Néel theory of ferrimagnetism, Am. J. Phys. 23 (1955) 356–370.

[27] C.G. Shull, E.O. Wollan, W.C. Koehler, Neutron scattering and polarization by ferromagnetic materials, Phys. Rev. 84 (1951) 912–921.